広島大学学位請求論文

Targeted gene editing in the sea urchin embryo using zinc-finger nucleases

(ジンクフィンガーヌクレーゼを利用したウニ胚における
標的遺伝子の編集)

2011 年

広島大学大学院理学研究科
数理分子生命理学専攻

落合　博

目次

1. 主論文

Targeted gene editing in the sea urchin embryo using zinc-finger nucleases
(ジンクフィンガーヌクレーゼを利用したウニ胚における標的遺伝子の編集)

2. 公表論文

Targeted mutagenesis in the sea urchin embryo using zinc-finger nucleases.
Ochiai, H., Fujita, K., Suzuki, K., Nishikawa, M., Shibata, T., Sakamoto, N. & Yamamoto, T.
Genes to Cells, 15, 875-885, 2010.

3. 参考論文

(1) Analysis of *cis*-regulatory elements controlling spatio-temporal expression of *T-brain* gene in sea urchin, *Hemicentrotus pulcherrimus*.
Ochiai, H., Sakamoto, N., Momiyama, A., Akasaka, K. & Yamamoto, T.
Mechanisms of Development, 125, 2– 17, 2008.

(2) The *Ars* insulator facilitates *I-SceI* meganuclease-mediated transgenesis in the sea urchin embryo.
Ochiai, H., Sakamoto, N., Suzuki, K., Akasaka, K. & Yamamoto, T.
Developmental Dynamics, 237, 2475–2482, 2008.

(3) Suppressor of Hairless (Su(H)) is required for foregut development in the sea urchin embryo.
Karasawa, K., Sakamoto, N., Fujita, K., Ochiai, H., Fujii, T., Akasaka, K. & Yamamoto, T.
Zoological Science, 26, 686-690, 2009.

(4) Role of the nanos homolog during sea urchin development.
Fujii, T., Sakamoto, N., Ochiai, H., Fujita, K., Okamitsu, Y., Sumiyoshi, N., Minokawa, T. & Yamamoto, T.
Developmental Dynamics, 238, 2511–21, 2009.

(5) Dicer is required for the normal development of sea urchin, *Hemicentrotus pulcherrimus.*
Okamitsu, Y., Yamamoto, T., Fujii, T., Ochiai, H. & Sakamoto, N.
Zoological Science, 27, 477-486, 2010.

主論文

Targeted gene editing in the sea urchin embryo using zinc-finger nucleases

Hiroshi Ochiai

2011

Contents

Introduction

Targeted gene editing, such as targeted mutagenesis and targeted gene addition, is a powerful approach to examine the function of genes and the regulatory mechanism for their expression during animal development. However, this approach is available only in limited animal models, such as the mouse, in which embryonic stem (ES) cells required for gene targeting have been established. In other animal models in which a gene editing approach is not available, to analyze the function of a gene of interest, loss-of-function approaches, such as the introduction of small interfering RNA and/or morpholino antisense oligonucleotide (MO) that reduce the production of the encoded protein, are employed as alternatives to targeted mutagenesis (Nasevicius et al., 2000; Harborth et al., 2001). However, it has been reported that, in many cases, the complete inactivation of a gene of interest is not achieved by these loss-of-function approaches (so-called gene knockdown) (Cost et al., 2010). In animal models in which a gene editing approach is available, targeted gene addition enables *in vivo* monitoring of the expression of the endogenous gene of interest and aids in examining the regulatory mechanism of its expression. On the other hand, in animal models in which a gene editing approach is not available, the random introduction of a reporter construct that contains *cis*-regulatory elements of the gene of interest is used as an alternative to targeted gene addition to gain insights into the regulatory mechanism of gene expression. However, it has been reported that the expression profile of the randomly integrated reporter gene might be affected by the chromosomal environment (Levis et

al., 1985). Accordingly, for the quantitative analysis of gene expression, insertion of a reporter gene into the specific genomic locus of interest is used in model organisms in which a gene editing approach is available (Elowitz et al., 2002; Yoo et al., 2004; Raser et al., 2004). Therefore, the development of novel strategies to further targeted mutagenesis and targeted gene addition in different model organisms is required.

Recently, a new method for targeted mutagenesis using engineered zinc-finger nucleases (ZFNs) has been used in *Drosophila* (Beumer et al., 2008), zebrafish (Doyon et al., 2008; Meng et al., 2008; Foley et al., 2009), plants (Shukla et al., 2009; Townsend et al., 2009) and human cultured cells (Urnov et al., 2005; Hockemeyer et al., 2009; Zou et al., 2009). ZFNs consist of a customized array of zinc fingers (ZFs) that bind to a specific DNA sequence and the nuclease domain of the restriction enzyme FokI. When two ZFNs bind to their associated target sequences in the appropriate direction, the nuclease domains dimerize and a double-stranded break (DSB) is introduced. The ZFN-induced DSB can then be repaired with high efficiency either by homology-directed repair (HDR) or by error-prone nonhomologous end joining (NHEJ) repair independent of a DNA template for repair. ZFNs, therefore, induce a site-specific insertion or deletion at the DSB site after NHEJ repair (Doyon et al., 2008; Maeder et al., 2008). In the zebrafish, co-injection of mRNAs for ZFNs whose target site is positioned in the kinase insert domain receptor, *kdr* gene, into one-cell-stage zebrafish embryos led to mutagenic lesions at the target site and the mutations were transmitted through the germ line with high frequency (Meng et al., 2008). Alternatively, ZFNs can produce defined genetic modifications that include insertion of a reporter gene near the

site of the DSB by HDR using an exogenous targeting donor construct (Moehle et al., 2007; Beumer et al., 2008; Shukla et al., 2009). In the human cultured cells, it has been reported that the X-linked severe combined immune deficiency mutation in the interleukin-2 receptor-γ (*IL2RG*) gene was efficiently modified by ZFN-mediated gene correction (Urnov et al., 2005). It has been noted that, in animals, ZFN-induced DSBs are mainly repaired by NHEJ, so ZFN-mediated targeted gene correction and addition are considered to be challenging (Beumer et al., 2008; Meyer et al., 2010). In addition, because of the complexity of DNA sequence recognition by a ZF array, screening for ZFNs that introduce DSB at a specific genomic site is laborious. Consequently the application of targeted gene editing using ZFNs is not widespread.

The sea urchin embryo, which is transparent, simple and readily accessible to experimental perturbations using MO, offers a unique opportunity to study the regulation of morphogenesis during early development (McClay et al., 1992; Hardin, 1996). However, since the concentration of injected MO might be reduced through successive cell divisions, it was suggested that inactivation of the gene of interest could become insufficient at later stages of development. Therefore, alternatives to the knockdown approach using MO are required for the functional analyses of genes that are expressed at later stages in sea urchin development. In sea urchin embryos, some of the regulatory mechanisms underlying the expression of the genes involved in endomesoderm specification have been analyzed by means of the microinjection of reporter gene constructs that were randomly integrated into the genomic DNA (Makabe et al., 1995; Revilla-i-Domingo et al., 2004; Ransick & Davidson, 2006; Ochiai et al.,

2008a). Additionally, because of its transparency and small size, *in vivo* quantitative imaging methodology at cellular level has been established in this organism (Damle et al., 2006). However, because of the unavailability of targeted gene addition, quantitative imaging analysis has been limited to examine the expression of exogenous reporter genes that, as mentioned above, might be quantitatively different from the expression of endogenous genes.

In this thesis, to establish a system of targeted mutagenesis and targeted gene addition in the sea urchin, I applied ZFN technology to the sea urchin, *Hemicentrotus pulcherrimus.* To generate functional ZFNs, I adopted a bacterial one-hybrid (B1H) system using ZF randomized libraries (Meng et al., 2008) and a single-strand annealing (SSA) assay using cultured cells. Using these screenings, I selected a pair of ZFNs targeting *HpHesC*, the *H. pulcherrimus* homologue of *HesC*, which was reported to repress several transcription factor genes responsible for the differentiation of primary mesenchyme cells (PMCs) in the sea urchin embryo (Revilla-i-Domingo et al., 2007; Yamazaki et al., 2009). I have shown the efficacy of the ZFNs by injecting them into sea urchin embryos and performing sequence analysis to identify mutations in the *HpHesC* gene in the injected embryos. Moreover, I have demonstrated that the insertion of a reporter cassette into a specific genomic locus was successfully achieved by injecting another pair of ZFNs for *HpEts* gene, which encodes an Ets transcription factor, along with a targeting donor construct. I have also shown that the introduction of mRNA for a dominant negative form of *HpLig4*, a gene that encodes the *H. pulcherrimus* homologue of the DNA ligase IV required for NHEJ, increased the

efficiency of ZFN-mediated targeted gene addition. These results suggest that targeted gene editing using ZFNs is feasible in sea urchin.

Experimental Procedures

Determination of the cDNA sequence of HpHesC and HpLig4

The cDNA of *HpHesC* and of the region of the *Hemicentrotus pulcherrimus* homologue of DNA ligase IV (*HpLig4*) that encodes the carboxy-terminal tandem BRCT repeat (DN-lig4) were amplified by PCR from a cDNA library using primers for *HpHesC* (HpHesCF and HpHesCR) (Table 1) and *HpLig4* (CTlig4F and CTlig4R) (Table 1), respectively. The amplified cDNA was subcloned into pBluescriptII SK(+) (Stratagene), and the nucleotide sequence was determined using a CEQ 8000 Genetic Analysis System (Beckman Coulter). The nucleotide sequence of *HpHesC* cDNA was deposited in GenBank (Accession No. GU390551).

Confirmation of genetic variations in the target gene locus

Genomic DNA was extracted from the tube feet of adult *H. pulcherrimus*. Regions of 153 bp in the third exon of the *HpHesC* gene was amplified from the genomic DNA using a primer sets for *HpHesC* target site (HT1F and HT1R). The amplified genomic DNA fragments were sequenced directly.

Construction of randomized ZF libraries and B1H selection

Construction of the zinc-finger randomized libraries and B1H selections were carried out as described by Meng & Wolfe (2006) with some modifications. In these

experiments, ZF randomized libraries, which express fusion proteins consisting of three-finger ZF arrays and the omega subunit of RNA polymerase, and HIS3 reporter vectors, which contain the target sequences for the ZF arrays, were cotransfected into the US0*ΔhisBΔpyrFΔrpoZ* bacterial strain and plated on histidine-deficient plates with the HIS3 inhibitor 3-amino-1,2,4-triazole (3-AT) (Fig. 1A).

To construct the randomized ZF libraries, randomized sequence-receptive vectors were constructed by modification of pc3XB-ZF70, a ZF module encoding a vector for restriction digestion-based modular assembly (Wright et al., 2006; ZF Consortium Modular Assembly ZF Set (Addgene)). Briefly, two BbsI sites were introduced into pc3XB-ZF70 by inverse PCR to insert a randomized ZF cassette for a recognition helix and ZF-specific mutations to enable PCR-based modular assembly. The first, second and third modules from the N-terminus were designated ZF1-BbsI, ZF2-BbsI and ZF3-BbsI, respectively (Fig. 1B). ZF-specific mutations were also introduced into pc3XB-ZF64 and pc3XB-ZF63 (ZF module-encoding vectors; ZF Consortium Vector Kit v1.0) by inverse PCR (Fig. 1B). pc3XB-ZFA36, which encodes a three-finger ZF protein comprised of ZF60, ZF64 and ZF63 from the N-terminus (Ramirez et al., 2008; Table 2), was constructed by restriction digestion-based modular assembly as described previously (Wright et al., 2006). Furthermore, one of ZF60, ZF64 or ZF63 within ZFA36 was substituted to the ZF1-BbsI, ZF2-BbsI and ZF3-BbsI modules by restriction digestion-based modular assembly to construct pc3XB-Z1B, pc3XB-Z2B and pc3XB-Z3B, respectively (Table 2). DNA fragments encoding three ZFs within pc3XB-ZFA36, pc3XB-Z1B, pc3XB-Z2B and pc3XB-Z3B were amplified using the

oligonucleotide primers 3Z-F and 3Z-R (Table 1). The amplified fragments were digested with NotI and SpeI and inserted into the NotI/XbaI site of pB1H2ω2-zif268, which expresses a fusion protein of the DNA-binding domain of zif268 and the omega subunit of RNA polymerase in bacteria (Meng et al., 2008) to generate pB1H2ω2-ZFA36, pB1H2ω2-Z1B, pB1H2ω2-Z2B and pB1H2ω2-Z3B. A randomized sequence flanked by BbsI sites (Random+BbsI-L) was synthesized and converted to double-stranded DNA by primer extension with the Random+BbsI-S primer (Table 1) and KOD-plus- (TOYOBO). The randomized sequence was digested with BbsI and inserted into the BbsI sites of pB1H2ω2-Z1B, pB1H2ω2-Z2B and pB1H2ω2-Z3B to generate randomized libraries containing more than 2×10^9 types.

To construct a series of pH3U3-B1H derivatives as HIS3 reporter vectors for B1H selections, several sets of two complementary oligonucleotides corresponding to parts of the *HpHesC* and *HpEts* targets sequence (Table 3) were synthesized chemically, annealed and inserted into the EcoRI/XmaI site of pH3U3-mcs (Meng et al., 2008). To select the ZF recognizing each subsite of the *HpHesC* and *HpEts* target sequences, a first-stage library screening in the B1H system was carried out as described by Meng & Wolfe (2006). After this selection, pools of ZFs of positive clones were amplified with KOD-plus- from the pB1H2ω2-Z1B-derived library using ZF1-forward and ZF1-reverse primers, from the pB1H2ω2-Z2B-derived library using ZF2-forward and ZF2-reverse primers and from the pB1H2ω2-Z3B-derived library using ZF3-forward and ZF3-reverse primers (Table 1). The PCR products were analyzed by 1.5% agarose gel electrophoresis in Tris-borate-EDTA (TBE) buffer, and the appropriate bands were

excised and purified from the gel using a Gel Extraction Kit (Qiagen).

To construct a vector for the second stage of B1H selection, pB1H2ω2-ZFA36 was subjected to inverse PCR with pB1H2ω2-BbsI-F and pB1H2ω2-BbsI-R primers (Table 1), followed by insertion of a DNA fragment (5′–GCCTGAGTCTTC-(55bp)-GAAGACATAGAG–3′), which includes two BbsI sites at both ends. A library of three-finger ZF arrays was assembled from three pools of individual PCR-amplified ZFs by overlapping PCR (Fig. 1A) (Meng et al., 2008). Next, the purified PCR products were analyzed by 1.5% agarose gel electrophoresis in TBE buffer, and the band with appropriate sizes was excised and purified using the above-mentioned Gel Extraction Kit. The PCR-amplified three-finger ZF arrays were digested with BbsI and inserted into the BbsI sites of the vector to construct the ZF array libraries for the second-stage B1H selection. The second stage of selection was carried out using the ZF array libraries and pH3U3-B1Hs containing either an *HpHesC1* site (5′–GGGCGAGTCT–3′), *HpHesC2* site (5′–GGGGTCTGGA–3′), *HpEts1* site (5–GGGGTTGACG–3′) or *HpEts2* site (5–GATGATGACT–3′) (Fig. 1A). ZF array-positive clones were isolated from 20 mM 3-AT stringency plates, and the nucleotide sequences of the inserted cDNAs encoding the ZF arrays were analyzed.

SSA assay using HEK293T cells

To construct the pSTL vector as a ZFN expression vector for the SSA assay, the BsgI site of pST1374 (ZFN expression vector; ZF Consortium Vector Kit v1.0) was eliminated by inverse PCR with delta-BsgI-L and delta-BsgI-R primers (Table 1) and a

DNA region of pST1374 between the XbaI and EcoRI sites was substituted with a DNA fragment, pST (Fig. 1C). Next, the cDNAs of the ZF arrays selected by the B1H procedure were excised by digestion with XbaI and BsgI and inserted between the XbaI and BsgI sites to generate the pSTL-ZFN expression vector. This vector includes a 6-amino acid linker (TGAAAR) between the ZF DNA-binding domain and the FokI nuclease domain that restricts the nuclease activity to sites containing a 6-bp spacer (Shimizu et al., 2009).

pGL4-SSA reporter constructs containing a ZFN target sequence between the inactive fragments of the *luciferase* gene were generated using a pGL4 vector (Promega). PCR was conducted to amplify 5′ and 3′ fragments of the *luciferase* gene, including a 700-bp region of homologous overlap, using the following oligonucleotides as primers: SSA-luc2-1 and SSA-luc2-2 for the 5′ fragment and SSA-luc2-3 and SSA-luc2-4 for the 3′ fragment (Table 1). The *luciferase* gene of pGL4 was substituted into the amplified fragments that were joined to each other by introduced XmaI sites. The cytomegalovirus (CMV) immediate-early enhancer/promoter region was inserted into the upstream of the inactive *luciferase* gene. The following oligonucleotides were annealed and inserted between the BsaI sites of pGL4-SSA vector: SSA-GL4-C1C1-S and SSA-GL4-C1C1-A were used to generate pGL4-SSA-C1C1, SSA-GL4-C2C2-S and SSA-GL4-C2C2-A were used to generate pGL4-SSA-C2C2, SSA-GL4-C1C2-S and SSA-GL4-C1C2-A were used to generate pGL4-SSA-C1C2, SSA-GL4-Ets1-S and SSA-GL4-Ets1-A were used to generate pGL4-SSA-Ets1 and SSA-GL4-Ets2-S and SSA-GL4-Ets2-A were used to generate pGL4-SSA-Ets2 (Table 1).

HEK293T cells were grown in DMEM supplemented with 10% FCS. The cells were cotransfected with 200 ng of the pSTL-ZFN expression vector, 100 ng of the pGL4-SSA reporter plasmid and 20 ng of the pRL-CMV reference vector (Promega) using Lipofectamine 2000 (Invitrogen) in 96-well plates at 50,000 cells/well. After 24 h, dual-luciferase assays were conducted using the Dual-Glo luciferase assay system (Promega) in a TriStar LB 941 plate reader (Berthold) based on the manufacturer's instructions.

Construction of a targeting donor construct

A genomic region spanning 2410 bp (-1137 to +1273 from the stop codon of the *HpEts* gene) from sea urchin genomic DNA was amplified by PCR using Ets-HRD-F and Ets-HRD-R primers (Table 1) and subcloned into pBluescriptII SK(+) to construct a pBSK-Ets-HRD plasmid. Two oligonucleotides (2A-peptide-S and 2A-peptide-A) (Table 1) were synthesized and converted to double-stranded DNA by primer extension with KOD-plus-. The 2A-peptide coding DNA fragment was subcloned into the EcoRV site of pBluescriptII SK(+) and an *H2B-GFP* cassette (Fujii et al., 2009) was cloned downstream of the 2A-peptide coding sequence to generate pBSK-2A-H2B-GFP vector. A *2A-H2B-GFP* cassette was amplified by PCR with KOD-plus using 2A peptide-2F and T3 promoter primers (Table 1). To generate a targeting donor construct, pBSK-Ets-HRD was subjected to inverse PCR with Ets HRD-inv-F and Ets HRD-inv-R primers (Table 1), followed by insertion of the amplified *2A-H2B-GFP* cassette.

Sea urchin culture

Sea urchins (*H. pulcherrimus*) were harvested from Seto inland sea or Tateyama Bay, and their gametes were obtained by coelomic injection of 0.55 M KCl. Fertilized eggs were cultured in filtered seawater at 16 °C.

mRNA synthesis and microinjection

cDNAs encoding ZFNs and nuclear localization signal (NLS) - the carboxy-terminal tandem BRCT repeat of *HpLig4* (designated DN-lig4) were subcloned into a transcription vector containing a T7 promoter and the β-globin leader sequence. The plasmids containing ZFN or DN-lig4 cDNAs were linearized with restriction enzymes. HesC ZFN and Control ZFN mRNAs capped with $m^7G(5')ppp(5')G$ were synthesized using a mMESSAGE mMACHINE T7 Kit (Ambion). The polyadenylated *HpEts* ZFN and DN-lig4 mRNAs capped with anti-reverse cap analog were synthesized using a mMESSAGEmMACHINE T7 ultra kit (Ambion). An MO complementary to the sequence containing the translation start site of *HpHesC* mRNA (5′–ATGCTTACTTCATCTGGATACCAAC–3′) and a standard control MO (5′–CCTCTTACCTCAGTTACAATTTATA–3′) were obtained from Gene Tools. The MOs and mRNAs were dissolved in 10% glycerol. Microinjection was carried out as described by Rast (2000) with some modifications by Ochiai et al. (2008a). Two or four picoliters of the solution was injected into each fertilized egg. To observe the phenotypes, embryos were fixed in filtered seawater containing 0.01% formaldehyde.

Quantitative PCR

Quantitative PCR was conducted as described previously (Ochiai et al., 2008b) using qHpDelta-F and qHpDelta-R primers (Table 1).

Whole mount in situ hybridization

Whole mount in situ hybridization was carried out following the method in Minokawa et al. (2004). Digoxigenin-labeled RNA probes for *HpDelta* were prepared using T3 or T7 RNA Polymerases (Roche) with a DIG RNA Labeling Mix (Roche).

Sequence analysis of mutations

Genomic DNAs were isolated from approximately 300 control noninjected embryos and approximately 300 embryos injected with 10 pg each of *HpHesC* ZFN mRNAs at different developmental stages. A 153-bp PCR fragment containing the target sequence for the HpHesC ZFNs was amplified by PCR using the HT1F and HT1R as primers. The PCR products derived from genomic DNA from *HpHesC* ZFN mRNA-injected embryos at 8 h postfertilization (hpf) were purified using QIAquick PCR Purification Kit (Qiagen) and subcloned into pBluescript II SK+ (Stratagene). The nucleotide sequences of the clones were analyzed to determine the types of mutations around the *HpHesC* ZFN target site. Aliquots (200 ng) of the PCR products were digested with BslI (New England Biolabs) overnight, purified and analyzed by 3% agarose gel electrophoresis.

Genomic PCR analysis

Forty fg of the targeting donor construct alone or in combination with 1 pg of each *HpEts* ZFN mRNA were injected into fertilized sea urchin eggs. Genomic DNAs were isolated from 300 control noninjected embryos, 300 donor-injected embryos and 300 co-injected embryos at 24 hpf using DNeasy Blood & Tissue Kit (Qiagen). PCR was performed with KOD-plus- using extracted genomic DNA and with 0.3 μM of gene specific primers for *HpArs* (Ochiai et al., 2008a) for 25 cycles (94°C 15 sec, 60°C 15 sec, 68°C 1 min) or for confirmation of targeted gene addition (primer1 and 2) (Table 1) for 37 cycles (94°C 30 sec, 65°C 30 sec, 68°C 4 min). PCR products for *HpArs* and confirmation of targeted gene addition were separated on 2% and 1% agarose gels, respectively.

Reverse transcription PCR analysis

Total RNA was extracted from approximately 300 control noninjected embryos, approximately 300 embryos injected with 40 fg of the targeting donor construct, approximately 300 embryos injected with 40 fg of the targeting donor construct and 1pg of *HpEts* ZFN mRNA and approximately 300 embryos injected with 40 fg of the targeting donor construct and 1pg of *HpEts* ZFN mRNA in combination with 5 pg of DN-lig4 mRNA at 24 hpf using ISOGEN (NIPPONGENE, Japan) as described in the manufacturer's manual. The cDNAs were prepared by using a ThermoScript RT-PCR System (Invitrogen) with random hexamers following the manufacturer's instructions. Targeted gene additions were detected by the following PCR with KOD-plus- using 0.3

μM of primers (primer3 and primer4) (Table 1) for 35 cycles (94°C 30 sec, 60°C 30 sec, 68°C 4 min). As a control, *mitochondrial cytochrome oxidase subunit I* (*HpMitCOI*) mRNA, which is expressed constitutively at the same level during sea urchin development (Okabayashi & Nakano, 1983; Yamaguchi & Ohba, 1994; Fujiwara & Yasumasu, 1997) was detected by PCR using reaction mixtures containing 0.3 μM of *HpMitCOI*-specific primers (Ochiai et al., 2008a) for 23 cycles (94°C 15 sec, 60°C 15 sec, 68°C 1 min). The PCR products for the targeted gene insertion and for *HpMitCOI* were separated on 1% and 2% agarose gels, respectively.

Live imaging of sea urchin embryos

Injected embryos were reared in 35-mm tissue culture dishes and allowed to develop to the late gastrula stage (30 hpf). Embryos were then mounted in a microchamber assembled as follows: (i) High vacuum grease (DOW CORNING) was applied at the corners of a square 15 mm wide on a 35-mm glass based dish (Iwaki): (ii) Approximately 100 embryos were mouth-pipetted onto the center of the glass surface: (iii) The microchamber containing the embryos was closed with a 18 x 18-mm #1 coverslip (Matsunami): (iv) The corners of the coverslip were gently pressed to squeeze and the immobilize swimming embryos: and (v) The microchamber was filled with filtered sea water and sealed with mineral oil (Sigma-Aldrich). The embryos were visualized on IX-81 fluorescence microscope (Olympus) equipped with MetaMorph software (Universal Imaging).

Statistical analysis

Data are presented as means ± SD. Differences were evaluated for significance by Student's *t*-test, with significance defined as values of $P < 0.01$ using a two-tailed unpaired *t*-test.

Results

Generation of functional ZFNs targeting the HpHesC gene

To evaluate the functionality of the engineered ZFNs in the sea urchin, I generated ZFNs targeting the *HpHesC* gene. The sea urchin *HesC* gene, which is expressed in the whole embryo except for the micromere lineage during early embryogenesis, represses several transcription factor genes that are responsible for PMC differentiation (Revilla-i-Domingo et al., 2007; Yamazaki et al., 2009). When this gene is repressed at the translational level by an MO, the number of PMCs increases (Revilla-i-Domingo et al., 2007). First, I cloned a cDNA for *HpHesC* and determined its nucleotide sequence. The HpHesC protein was predicted to have a basic helix-loop-helix DNA-binding domain and a Hairy Orange domain. Therefore, I designed ZFNs targeting a site between these two conserved domains. If an NHEJ-mediated mutation was introduced at the target site by ZFNs, I expected that the function of the *HpHesC* gene would be disrupted (Fig. 2). In the genomic sequence of *Strongylocentrotus purpuratus*, which is closely related to *H. pulcherrimus*, a nucleotide sequence identical to the target site (5'–TCCAGACCCCNNNNNNGGGCGAGTCT–3') was found only in the *SpHesC* gene. However, single nucleotide polymorphisms (SNPs) can be detected in the coding region as well as the intron in the *H. pulcherrimus* gene (Yamamoto et al., 2007). Therefore, to confirm that no SNPs were present in the target site, I examined the genetic variations in the target sequence of the *HpHesC* gene. No polymorphisms were found for *H.*

pulcherrimus in the target site (data not shown).

To generate three-finger ZFNs targeting the *HpHesC* gene, I adopted the directed domain shuffling and B1H system described by Meng et al. (2008) with some modifications (Fig. 1A). The Cys_2His_2 ZF domain, which consists of approximately 30 amino acid residues, recognizes a target subsite that consists of 3 or 4 bp within its recognition helix (Wolfe et al., 2000). In the engineering strategy, highly specific three-finger ZF arrays recognizing 9 or 10 bp were selected from the libraries, in which each recognition helix had been randomized (codon encoded VNS in which V represents A, C or G, N represents A, C, G or T and S represents G or C, see Experimental Procedures for details). The framework involving sequences outside the recognition helix in the ZF domain was reported to be involved in structural stability (Shi & Berg 1995). Therefore, to construct ZF randomized libraries, I adopted the Sp1C consensus framework, which has been shown to have enhanced stability toward chelating agents (Shi & Berg 1995; Mandell & Barbas 2006). In addition, many species of designed ZFs that recognize DNA triplets have been generated using this framework (Segal et al. 1999; Dreier et al., 2000, 2001, 2005).

After two rounds of screening with the randomized libraries (Fig. 1A, see Experimental Procedures for details), I obtained 10 cDNA clones for three-finger ZF arrays targeting the *HpHesC1* site (5'–GGGGTCTGGA–3') and 30 cDNA clones for three-finger ZF arrays targeting the *HpHesC2* site (5'–GGGCGAGTCT–3'). I determined the nucleotide sequences of 10 cDNA clones of each type. Alignment of the predicted amino acid sequences of the recognition helices in the ZF arrays showed that

some residues in the recognition helix occurred frequently (Fig. 3). For example, the +6 residues in the second recognition helix of the *HpHesC1*-binding ZF array clones were all arginine residues.

Next, to screen for functional ZFNs, ZFN expression constructs were generated by fusion of the cDNAs for the selected ZF arrays and a nuclease domain of FokI, and an SSA assay was carried out (Szczepek et al., 2007). In the SSA assay, a ZFN construct and a reporter construct, in which the *luciferase* gene is split into two inactive fragments separated by both insertion of a stop codon and a pair of target sites for either *HpHesC1* or *HpHesC2*, were cotransfected into cultured cells. When a DSB at the target site is induced by the ZFN homodimers, SSA occurs between the homologous regions of the inactive fragments, producing an active *luciferase* gene (Fig. 4A). As shown in Fig. 4B, the individual ZFNs for *HpHesC1* or *HpHesC2* showed different levels of reporter activity as homodimers. However, some ZFNs had low levels of activity in the SSA assay (Fig. 4B), although all the selected ZF arrays possessed the potential to bind to *HpHesC* sites. In the assayed samples, clone C1-4 for the *HpHesC1* site and clone C2-2 for the *HpHesC2* site showed the highest activities. To examine the activity of ZFNs as heterodimers, an SSA reporter vector containing both *HpHesC1* and *HpHesC2* sites was prepared and the SSA assays were carried out using the C1-4 and C1-8 clones for the *HpHesC1* site, which showed the highest and lowest activities as homodimers, respectively (Fig. 4B), and the C2 clones for the *HpHesC2* site (Fig. 4C). Consistent with the activity of the ZFNs as homodimers, the combination of clone C1-4 for the *HpHesC1* site and clone C2-2 for the *HpHesC2* site showed the highest activity among

combinations examined. I referred to these ZFNs as HpHesC1 ZFN and HpHesC2 ZFN and used them for use in further experiments.

Effects of injecting mRNAs for the ZFNs targeting the HpHesC gene into sea urchin embryos

It has been reported that the FokI nuclease domain variants RR and DD have a reduced their propensity for homodimerization, thereby decreasing the frequency of off-target cleavage events through homodimerization of an individual ZFN (Szczepek et al., 2007). Therefore, the nuclease domains of HpHesC1 ZFN and HpHesC2 ZFN were mutated to DD and RR versions, respectively, generating $HpHesC1_{DD}$ and $HpHesC2_{RR}$ ZFNs.

To validate the functionality of ZFNs in sea urchin embryos, *HpHesC* ZFN mRNAs or *HpHesC* MO, which target the translation start site of *HpHesC* mRNA, were injected (Fig. 5). In the embryos injected with *HpHesC* MO, an increase in the number of PMCs in the blastocoel was observed at 24 hpf (Fig. 5C) consistent with a previous report for *S. purpuratus* (Revilla-i-Domingo et al., 2007). In this thesis, this phenotype is called the *HpHesC* morphant phenotype. In the embryos injected with 6.5 pg each of the $HpHesC1_{DD}$ and $HpHesC2_{RR}$ ZFN mRNAs, most developed normally to the early gastrula stage, although some embryos showed the *HpHesC* morphant phenotype (Fig. 5B). When 13 pg each of the *HpHesC* ZFN mRNAs were injected, the *HpHesC* morphant phenotype was observed in 9.5% of the ZFN-injected embryos, but severely malformed embryos were also observed (Table 4). To verify whether the observed effects were *HpHesC* ZFN mRNA-specific, I prepared a control set of three-finger

ZFNs targeting 5'–GCGGCCAGGG–3' and 5'–GGTGTCCATG–3'. The target sequence for these control ZFNs, 5'–CCCTGGCCGCNNNNNNGGTGTCCATG–3', was not found in the genomic sequence of *S. purpuratus*. When 13 pg of each of the control ZFN mRNAs were introduced into sea urchin eggs, most embryos developed normally and no embryos with the *HpHesC* morphant phenotype were observed (Fig. 5A, Table 4). These findings indicate that the *HpHesC* morphant phenotype was induced by the introduction of the *HpHesC* ZFN mRNAs.

To confirm that the *HpHesC* morphant phenotype found in the embryos injected with *HpHesC* ZFN mRNAs was caused by disruption of the *HpHesC* gene, the expression of the *Delta* gene, which was reported to be down-regulated by HesC in *S. purpuratus* (Revilla-i-Domingo et al., 2007), was analyzed at 15 hpf by quantitative PCR. In embryos injected with both the $HpHesC1_{DD}$ and $HpHesC2_{RR}$ ZFN mRNAs, the amount of *HpDelta* mRNA was significantly increased compared with that in embryos injected with the $HpHesC1_{DD}$ or $HpHesC2_{RR}$ ZFN mRNA alone (Fig. 5D). The expression of *HpDelta* mRNA was also examined at 12 hpf by whole mount in situ hybridization. In embryos injected with control ZFN mRNAs, *HpDelta* mRNA expression was observed in the presumptive PMCs at the vegetal pole (Fig. 5E). In embryos injected with *HpHesC* ZFN mRNAs, although most embryos showed the *HpDelta* mRNA expression in presumptive PMCs as observed in control ZFN mRNA-injected embryos, in some embryos an expansion of mRNA expression at the vegetal pole and ectopic expression in ectoderm was observed (Fig. 5F).

Next, I analyzed the mutations introduced into the *HpHesC* target site by the

ZFNs (Fig. 6). DNA fragments amplified by PCR using genomic DNA extracted from *HpHesC* ZFN mRNA-injected embryos at 8 hpf were subcloned and their nucleotide sequences were determined (Fig. 6A). Among the 34 clones examined, deletions (17 clones, 50%) and insertions (four clones, 12%) were observed. In some of the clones that had deletions, substitutions were also observed. Overall, 44% of the *HpHesC* genes were disrupted by frameshifts. These results indicated that the endogenous *HpHesC* gene was disrupted by ZFN-induced site-specific mutagenesis in these sea urchin embryos.

To examine when the introduction of mutations by ZFNs occurred during the sea urchin development, DNA fragments amplified by PCR using genomic DNA extracted from *HpHesC* ZFN mRNA-injected embryos and control embryos at several stages of development were digested with the restriction enzyme BslI, which has two recognition sites in the target site for the *HpHesC* ZFNs (Fig. 6B). The DNA fragments derived from the control embryos were cut completely by BslI at all developmental stages (Fig. 6B). In contrast, a BslI-resistant fragment was faintly observed among the DNA fragments from the *HpHesC* ZFN mRNA-injected embryos at 4 hpf (eight-cell stage) and the amount of this fragment increased from 8 hpf (morula stage) to reach a plateau at 12 hpf (unhatched blastula stage) (Fig. 6B). These findings suggest that the ZFN-mediated mutations were introduced mainly between the eight-cell and unhatched blastula stages.

Necessity of the SSA assay for selection of functional ZFNs

Although B1H-selected ZF arrays have the potential to bind to their target sites, some ZFNs showed low activities in the SSA assays (Fig. 4B). To investigate if these differences in activity in the SSA assay originate from the functional differences of ZFNs, several mRNAs for ZFNs that show higher (C1-4, C2-1 and C2-2) or lower activities (C1-8 and C2-7) in the SSA assay were injected in different combinations into sea urchin eggs. PCR-based analysis was then performed using genomic DNA extracted from the injected embryos at 14 hpf (Fig. 6C). In agreement with the ZFN activities observed in the SSA assay, mutations at the *HpHesC* target site were more efficiently introduced in the sea urchin embryos by the injection of clone C1-4 for the *HpHesC1* site in combination with clone C2-2 for the *HpHesC2* site than by the injection of clone C2-1 (Figs 4C and 6C). This suggests that the activities of the ZFNs in the SSA assay are consistent with their activity in the sea urchin embryos and supports the proposal that functional ZFN clones can be selected by the SSA assay. Taken together, the results suggest that, subsequent to B1H selection, the SSA assay can be used to efficiently generate functional ZFNs.

Targeted gene addition into the HpEts locus using ZFNs

Recently, in mouse zygotes, targeted gene addition was achieved by the introduction of ZFN mRNAs with a targeting donor construct (Meyer et al., 2010). This prompted me to explore the possibility of inserting a reporter cassette into a genomic site of interest in the sea urchin embryos. To explore this further, *HpEts* ZFNs, whose target site (5'–

CGTCAACCCCNNNNNNGATGATGACT–3') is located immediately upstream of the stop codon of the *HpEts* gene, were selected by B1H and SSA screening (Fig. 7A). The Ets transcription factor, coded for by the *HpEts* gene, is expressed in PMCs and secondary mesenchyme cells (SMCs) at late gastrula stage (Kurokawa et al., 1999; Rizzo et al., 2006). These ZFNs are subsequently referred to as HpEts1 and HpEts2 ZFNs. The FokI nuclease domains of the HpEts1 and HpEts2 ZFNs were mutated to *sharkey* RR and *sharkey* DS variants, respectively, because they were recently reported to have enhanced cleavage activities (Guo et al., 2010). A targeting donor construct with approximately 1-kb homology arms containing a *2A-histone H2B-GFP* cassette (2A is a self cleaving peptide sequence, Szymczak et al., 2004), was also generated (Fig. 7A). Therefore, insertion of the reporter cassette into the *HpEts* locus is expected to result in the expression of two proteins: a fusion protein comprising the full length of HpEts fused to the 17 amino acid sequence of the 2A peptide; and H2B-GFP, which localizes to cell nuclei where its fluorescence can be more accurately quantified (Sprinzak et al., 2010). Both proteins are under the control of the endogenous *HpEts* promoter (Fig. 7A).

To validate the utility of ZFN-mediated targeted gene addition in the sea urchin, injections of the targeting donor construct with or without the *HpEts* ZFN mRNAs were carried out and genomic PCR analysis was performed using genomic DNA extracted from the embryos at 24 hpf (Fig. 7B). While, as expected, no PCR product was detected in the noninjected and donor-injected samples, a PCR product of the expected size was observed in the co-injected sample, suggesting that targeted gene addition was induced

by the introduction of ZFNs.

Recently, in *Drosophila*, although it was reported that HDR with a targeting donor construct is a minor event compared with error-prone NHEJ repair in wild-type flies, the efficiency of HDR with an exogenous donor construct was greatly enhanced in recipients deficient in the NHEJ component DNA ligase IV (Beumer et al., 2008), suggesting that inactivation of DNA ligase IV increases the efficiency of ZFN-mediated targeted gene addition. However, based on a microarray analysis, mRNA for *SpDnl4*, a gene that encodes the *S. purpuratus* homologue of DNA ligase IV, exists in sea urchin embryo immediately after fertilization (Sp-Dnl4, SPU_018243, http://urchin.nidcr.nih.gov/blast/exp.html), suggesting that the DNA ligase IV proteins may be maternally deposited in the egg and that inhibition of their function using MO may not work in the sea urchin embryos. Therefore, I cloned cDNA for the carboxy-terminal tandem BRCT repeat of DNA ligase IV (DN-lig4), the overexpression of which was reported to achieve a dominant-negative effect in human cultured cells (Wu et al., 2009), and examined the effect of DN-lig4 overexpression on the efficiency of ZFN-mediated targeted gene addition by reverse transcription (RT)-PCR analysis using RNAs that were extracted from injected embryos at 24 hpf (Fig. 7C). The expression of the *HpEts-2A-H2B-GFP* fusion gene was detected in the embryos into which *HpEts* ZFN mRNAs and the targeting donor construct were injected without DN-lig4 mRNA and the expression was significantly increased in the embryos into which *HpEts* ZFN mRNA and the targeting donor construct were coinjected in combination with DN-lig4 mRNA. This result suggests that introduction of DN-lig4

mRNA enhances the efficiency of ZFN-mediated targeted gene addition. Next, I examined H2B-GFP expression in the embryos into which *HpEts* ZFN mRNAs and the targeting donor construct were injected in combination with DN-lig4 mRNA using fluorescence microscopy at 30 hpf (late gastrula stage) (Fig. 7D–I). About 10 % of the injected embryos showed GFP expression in the nuclei of some PMCs and SMCs, in which *Ets* gene was reported to be expressed (Kurokawa et al., 1999; Rizzo et al., 2006).

Discussion

Generation of functional ZFNs by the combined use of B1H and SSA screenings

Recently, genetic manipulation using ZFN technology has been reported in several model organisms (Beumer et al., 2008; Doyon et al., 2008; Shukla et al., 2009; Zou et al., 2009). Despite its significance and utility, ZFN technology has not been widely used because the methods for generating functional ZFNs are considered to be very complicated. In this thesis, I successfully selected functional ZFNs by the combined use of a B1H system involving ZF randomized libraries and an SSA assay using cultured cells. In addition, I showed that targeted gene editing in sea urchin embryos was achieved using the selected ZFNs.

In this work, I selected several ZF arrays that bind to *HpHesC1*, *HpHesC2*, *HpEts1* and *HpEts2* target sites using B1H selection with ZF randomized libraries. It was reported earlier that individual ZF domains in a ZF array recognize their target subsites through the recognition helix (Wolfe et al., 2000). Among the selected ZF arrays, specific residues in the recognition helices were found to be correlated with specific bases in the target subsites. For example, when guanine was the first and second nucleotide from the 5' end of the subsite, arginine and histidine residues occurred most frequently at positions six and three, respectively of the recognition helices of the B1H-selected ZF arrays. The relationship between a specific base in the target subsite and amino acid residue in the recognition helix has been observed in natural ZF proteins and ZF arrays selected by phage display (Wolfe et al., 2000),

suggesting that I successfully selected appropriate ZF arrays by using B1H selection with randomized ZF libraries. However, there were several exceptions to these relationships among the frequent residues in the recognition helices of the B1H-selected ZF arrays. For example, when cytosine was the third nucleotide from the 5' end of the subsites, aspartic acid occurred most frequently at the -1 position in the second recognition helix from the N-terminal end of the B1H-selected ZF arrays that bound to the *HpHesC1* target site, whereas threonine was found most frequently at position -1 of the first recognition helix from the N-terminal end of the B1H-selected ZF arrays that bound to the *HpHesC2* target site. The mechanisms for DNA sequence recognition by ZF arrays are thought to be complex, because their specificities are affected by several factors, including sequence-dependent conformational flexibility of the DNA, and side chain-side chain interactions in the ZF array (Wolfe et al., 2000). Therefore, the interaction residues in the recognition helices were assumed to be determined by several factors, rather than a simple one-to-one interactions between specific positions on the helix and specific base-pairs in the ZF recognition site.

Although the B1H-selected ZF arrays possibly have the potential to bind to their target sequences, some ZFNs, which consist of both a B1H-selected ZF array and a nuclease domain of FokI, showed low activities in the SSA assay and the efficiency of mutagenesis using these ZFNs was also found to be low in the sea urchin embryos. Because DNA sequence recognition by ZF arrays is thought to be affected by several factors (Wolfe et al., 2000), it is also possible that the interaction between a ZF array and its fusion partner could affect the DNA-binding activity of the ZF array. Indeed, the

fusion partner of a ZF array in B1H selection is different from that in an SSA assay because, in the B1H selection, the omega subunit of RNA polymerase is used as the fusion partner of the ZF array while in the SSA assay, a nuclease domain of FokI is used. Thus, the fusion of a ZF array with the nuclease domain of FokI is likely to change the DNA-binding activity of the ZF array. Alternatively, the nuclease activity of a ZFN could be considered to decrease when the ZF array and the nuclease domain are fused. Thus, for efficient generation of highly functional ZFNs, the assessment of both the DNA-binding activity of ZF arrays by bacterial-based selection and the evaluation of ZFNs by the SSA assays are necessary.

Targeted mutagenesis in sea urchin embryos using ZFNs

The use of the ZFNs evaluated by the SSA assay was successful in introducing several types of mutations into a specific genomic site in sea urchin embryos. Most of these mutations were frameshift mutations that disrupted the *HpHesC* gene. However, because the target sites of the HpHesC ZFNs were designed to lie between the DNA-binding domain and the Hairy Orange domain, it is possible that the expression of the DNA-binding domain of HpHesC induces dominant-negative effects on the regulation of genes that are regulated by HesC. To examine this possibility, I injected an mRNA for the N-terminal DNA-binding domain of HpHesC into fertilized eggs and observed that these embryos did not show the *HpHesC* morphant phenotype and developed normally into pluteus larvae, suggesting that the N-terminal DNA-binding domain of HpHesC does not act in a dominant-negative manner (data not shown).

Regardless of the mutagenic frequency (44%), only 9.5% of the *HpHesC* ZFN mRNA-injected embryos showed the *HpHesC* morphant phenotype. Considering the finding that the introduction of ZFN-induced mutations mainly occurred between the eight-cell and hatched blastula stages in *HpHesC* ZFN mRNA-injected embryos, it is possible that this delay in the timing of the introduction of mutations may contribute to the difference in the rates of the genotype and phenotype incidences. In the sea urchin *S. purpuratus*, the expression of HesC begins at the morula stage (8 hpf) repressing the several of the transcription factor genes responsible for the differentiation of PMCs (Revilla-i-Domingo et al., 2007). Therefore, it is possible that the disruptions of *HpHesC* may occur after the stage when HesC exerts its functions. Another possibility is that only cell descendants in which both alleles of the *HpHesC* gene were disrupted exhibited the *HpHesC* morphant phenotype and cells in which only one allele of the *HpHesC* gene was disrupted in the ZFN mRNA-injected embryos did not show the phenotype.

Targeted gene addition in sea urchin embryos using ZFNs

Insertion of a reporter gene into a target site was detected by PCR-based analysis in embryos coinjected with the targeting donor construct and ZFN mRNAs. In embryos injected with the targeting donor alone, targeted gene addition was not observed. These results indicate that spontaneous homologous recombination is a rare event in the sea urchin and that ZFN-induced DSB at the target site stimulate HDR, resulting in an induction of targeted gene addition at a detectable level in agreement with earlier work

using different models (Beumer et al., 2008; Meyer et al., 2010). Moreover, introduction of DN-lig4 mRNA further increased the efficiency of ZFN-mediated targeted gene addition. It has been reported that DNA Ligase IV, a major component of the NHEJ pathway, forms a complex with XRCC4 and seals DNA ends (Wu et al., 2009) and that DSB repair is biased toward HDR by a disruption of the function of DNA ligase IV resulting in an increase in the efficiency of targeted gene modification (Beumer et al., 2008). Therefore, in the sea urchin, it is proposed that an inhibition of DNA ligase IV by introduction of DN-lig4 increases the propensity to repair ZFN-induced DSB through HDR, resulting in an enhancement in the efficiency of ZFN-mediated targeted gene addition. Although, in the *Lig4* mutant of *Drosophila*, DSB repair was reported to be almost completely biased toward HDR, the enhancement in the efficiency of ZFN-mediated targeted gene addition using DN-lig4 was modest in the sea urchin (Beumer et al., 2008). This may be because, when DSBs were introduced by ZFNs, DN-lig4 proteins are not translated at a rate high enough to completely inhibit the function of endogenous DNA ligase IV proteins. Therefore, the introduction of recombinant DN-lig4 and ZFN proteins into fertilized sea urchin eggs might considerably enhance the efficiency of ZFN-mediated targeted gene addition. The inhibition of NHEJ activity and the simultaneous enhancement of the activity of HDR may efficiently induce ZFN-mediated targeted gene addition in sea urchin embryos. It has been reported that overexpression of Rad51, a protein with homologous DNA pairing and strand exchange activities, increases the efficiency of gene targeting in human cells (Yáñez & Porter, 1999).

In sea urchin embryos, the injection of DN-lig4 mRNA did not induce any developmental abnormality until at least the 72 hpf pluteus stage (data not shown), suggesting that DNA ligase IV-dependent NHEJ is not necessary in the early development of the sea urchin. In mice, inactivation of DNA Ligase IV results in embryonic lethality as a consequence of massive apoptosis in the central nervous system (Frank et al., 2000), while *Drosophila* deficient for *Lig4* are viable and fertile and show no obvious signs of defects or other abnormalities (Gorski et al., 2003). These suggest that an enhancement in the efficiency of ZFN-mediated targeted gene addition through inactivation of DNA ligase IV may work only in a limited number of model organisms.

In conclusion, I have demonstrated here that functional ZFNs can be selected by the combined use of B1H and SSA screenings, and that using the selected ZFNs, targeted mutagenesis and targeted gene addition were achieved in sea urchin embryos. Moreover, I have shown that endogenous gene expression can be visualized by the insertion of a *2A-H2B-GFP* cassette into the *HpEts* locus in living sea urchin. These techniques provide useful tools for the analysis of the expression dynamics of endogenous genes during the development of sea urchin embryos that could be used in future work.

Figures

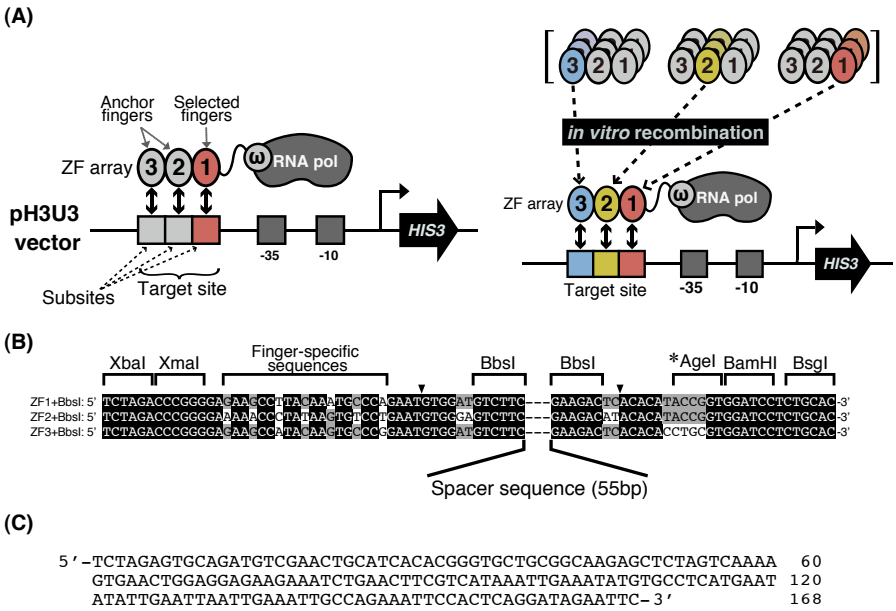

Figure 1. B1H screening and the construction of randomized ZF libraries. (A) Bacterial one-hybrid (B1H) screening. Schematic representations of the first selection stage of B1H screening to identify single zinc fingers (ZFs) with optimized binding to each 3-bp subsite within a recognition element is shown in the left panel. Schematic representations of *in vitro* recombination of individual zinc fingers and subsequent second selection stage against full ZF array recognition elements are shown on the right side of the panel. (B) Nucleotide sequences of randomized sequence-receptible modules, ZF1-BbsI, ZF2-BbsI and ZF3-BbsI. (C) Nucleotide sequence of DNA fragment pST.

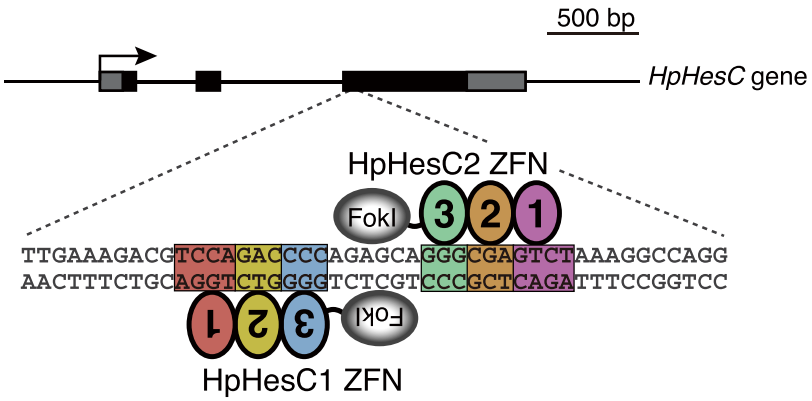

Figure 2. The *HpHesC* gene showing the ZFN target site. A schematic representation of the *Hemicentrotus pulcherrimus* homologue of the *HesC* gene (*HpHesC*) is shown. Exons are indicated by boxes. Gray and black boxes represent untranslated regions and coding regions, respectively. The bent arrow depicts the transcription start site. The ZFN-targeted sequence and the interaction site of a pair of the ZFNs used in this thesis are shown.

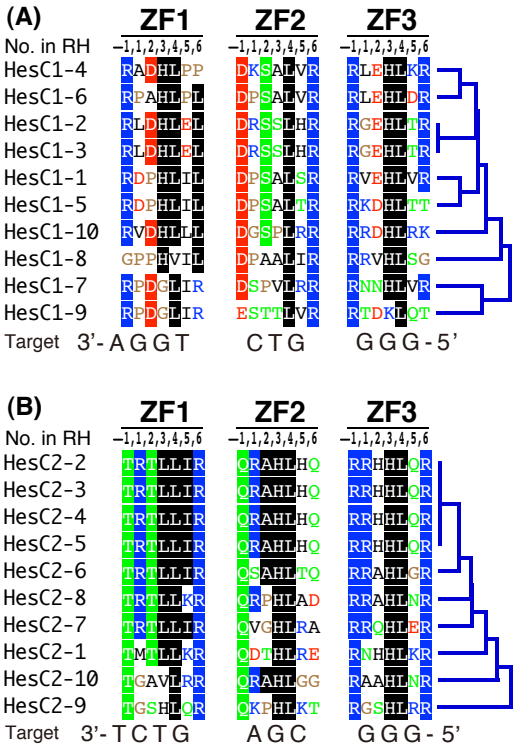

Figure 3. Alignment of the predicted amino acid sequences of the recognition helices in the selected ZF arrays. The predicted amino acid sequences of the recognition helices (residues −1 to +6) in the selected ZF arrays were aligned. Residues present in more than five of the clones are highlighted. The alignments shown in (A) and (B) were derived from selected clones for the *HpHesC1* (5'-GGGGTCTGGA-3') and *HpHesC2* (5'-GGGCGAGTCT-3') target sites, respectively. The numbers of residues in the recognition helix (No. in RH) and the target sequences are shown above and below each panel, respectively. The phylogenetic trees are shown on the right side of each panel.

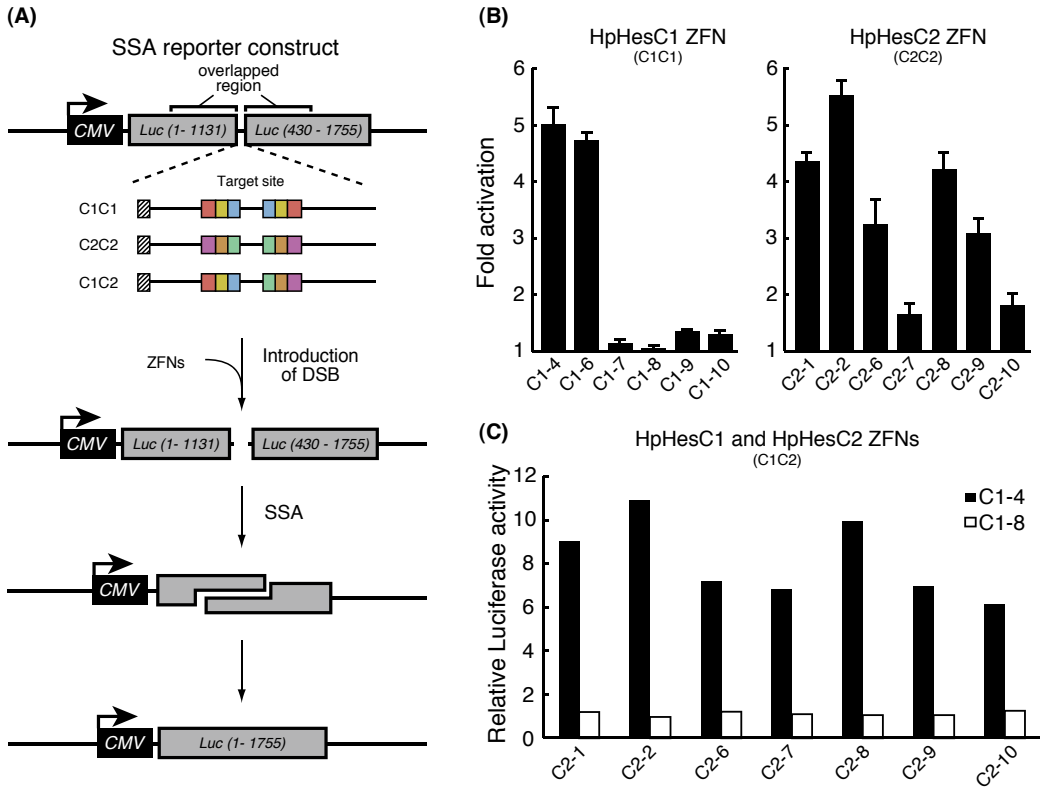

Figure 4. Evaluation of the functionality of engineered ZFNs using the SSA assays. For the dual-luciferase assay, HEK293T cells were transfected with three types of plasmids: a ZFN-expressing plasmid, a reporter plasmid and a reference plasmid. After transfection, the cells were incubated for 24 h, lysed and analyzed for their luciferase activity. (A) Schematic diagram of the SSA assay. The reporter plasmid encodes two split inactive parts of the *luciferase* gene with overlapping repeated sequences. Following a DSB caused by the ZFNs, a functional *luciferase* gene is generated by an SSA reaction. The hatched box represents a stop codon. (B) Cellular activities of the engineered ZFNs as homodimers. The fold activation of recombination by each ZFN represents the luciferase expression level in cells cotransfected with the ZFN vector, SSA reporter vector (either pGL4-SSA-C1C1 or pGL4-SSA-C2C2, see Experimental Procedures for details) and pRL-CMV reference vector compared with that in cells transfected with a control empty vector, SSA reporter vector and reference vector. Data are expressed as means ± SEM (n = 3). (C) Cellular activities of the engineered ZFNs as heterodimers. The expression level in cells cotransfected with SSA reporter vector (pGL4-SSA-C1C2, see Experimental Procedures for details), reference vector and indicated ZFN vector set was analyzed. The data were normalized to reference *Renilla* luciferase activity.

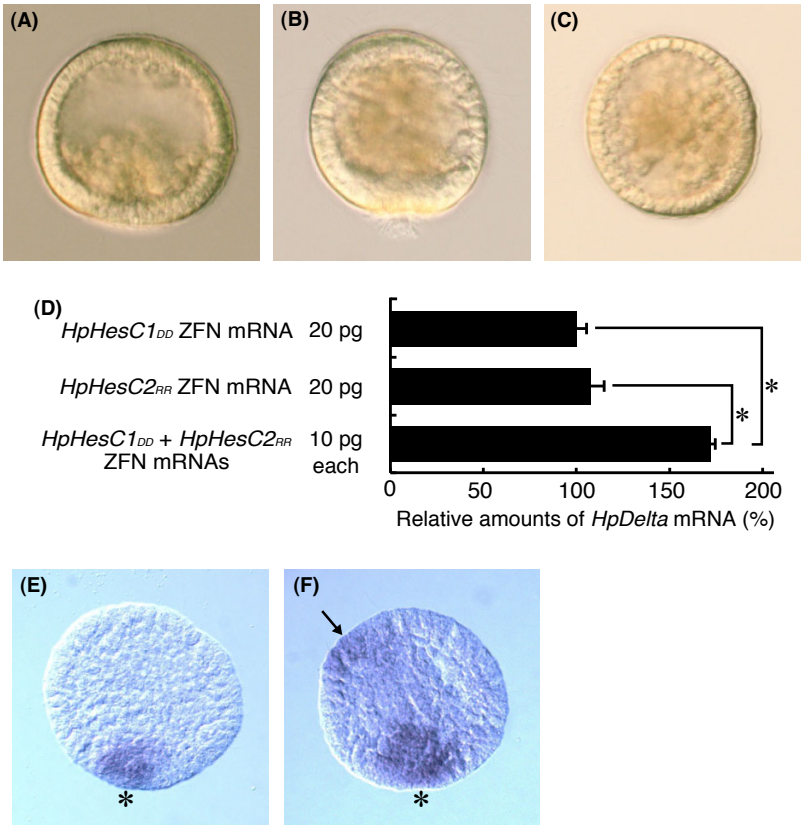

Figure 5. The effect of injection of *HpHesC* ZFN mRNAs into sea urchin embryos. (A–C) Bright-field images of embryos at 24 h postfertilization (hpf). (A) Control ZFN mRNA-injected embryo. (B) *HpHesC* ZFN mRNA-injected embryo. (C) *HpHesC* MO-injected embryo. Among the *HpHesC* ZFN mRNA-injected embryos, most embryos developed normally, although some embryos showed the *HpHesC* morphant phenotype (B). (D) Relative amounts of *HpDelta* mRNA in the sea urchin embryos injected with *HpHesC* ZFN mRNAs. The indicated amounts of ZFN mRNAs were injected into fertilized eggs. Total RNA was isolated from the embryos at 15 hpf, and *HpDelta* mRNA was analyzed by quantitative PCR. The expression levels in the ZFN mRNA-injected samples were normalized by those in the $HpHesC1_{DD}$ ZFN mRNA-injected samples. *P < 0.01, by Student's t-test. (E–F) Whole mount *in situ* hybridization showing the spatial expression of *HpDelta* mRNA at 12 hpf. (E) Control ZFN mRNA-injected embryo. (F) *HpHesC* ZFN mRNA-injected embryo. Arrow indicates *HpDelta* mRNA expression in ectoderm. Asterisk indicates the vegetal pole.

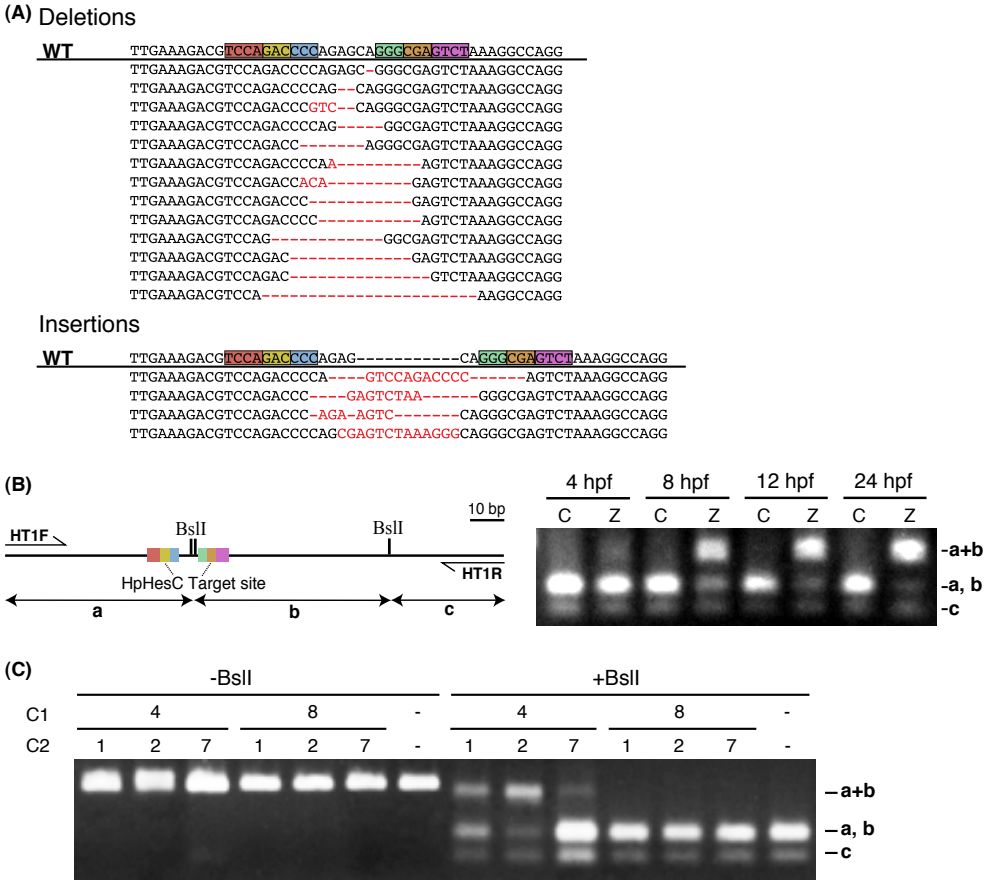

Figure 6. Analysis of the mutations induced by ZFNs. (A) Sequences from in sea urchin embryos injected with *HpHesC* ZFN mRNAs. The wild-type sequence is shown at the top with the ZFN-binding sites (boxed). Deletions are indicated by red dashes and insertions and substitutions are indicated by red letters. (B) A schematic representation of the *HpHesC* genomic region used for the PCR-based analysis is shown in the left panel. This region contains a target site for HpHesC ZFNs and three BslI sites. Two of the BslI sites are positioned in the middle of the *HpHesC* ZFN target site. In the right panel, a representative analysis of the PCR products during development is shown. The PCR products from genomic DNA of sea urchin embryos injected with *HpHesC* ZFN mRNAs (represented as Z) or control embryos (represented as C) were purified, digested with BslI and analyzed by agarose gel electrophoresis. The times of the genomic DNA extractions are shown at the top of the image. (C) The *in vivo* activity of several ZFN clones. The activity of the indicated combinations of C1 and C2 ZFNs was analyzed by the PCR-based analysis as described in (B). The genomic DNA was extracted at 14 h postfertilization.

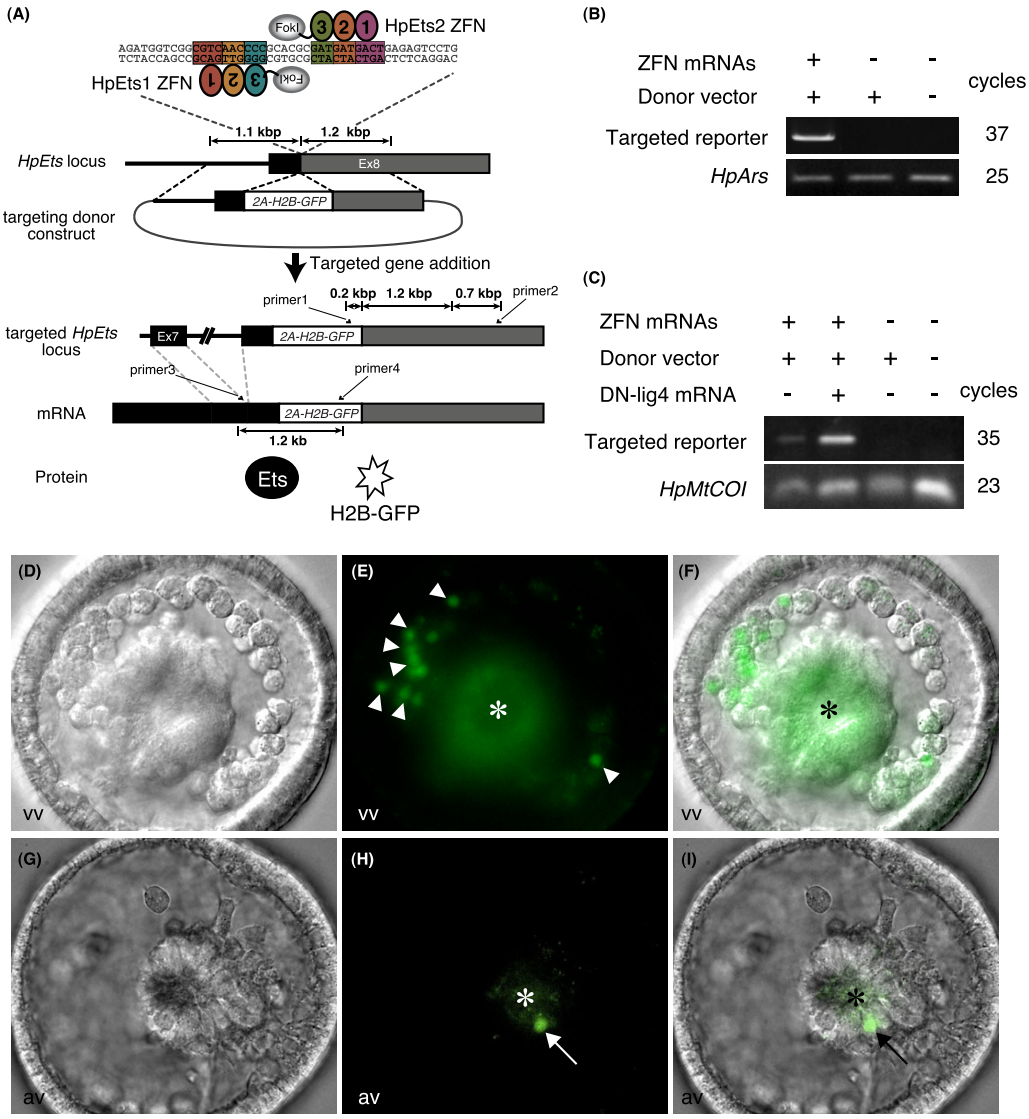

Figure 7. ZFN-mediated targeted gene addition. (A) The targeting donor construct for the insertion of *2A-histone H2B-green fluorescent protein* (*GFP*) cassette into the *HpEts* locus. The ZFN-targeted sequence and a pair of ZFNs for *HpEts* target site are shown. The structure of *HpEts* locus (part of intron 7 and exon 8) and the targeted *HpEts* allele is shown below. Gray and black boxes represent coding and non-coding exons, respectively. Schematic representation of the transcript and proteins, which are separated into the full length HpEts protein and H2B-GFP during translation in order to 2A self cleavage peptide, derived from the targeted *HpEts* allele are also shown. Primer sites for genomic PCR and reverse transcription-PCR (RT-PCR) analysis are indicated. (B) Representative results of PCR-based genotyping analysis of *HpEts* locus. PCR was performed using genomic DNA extracted from embryos, into which indicated samples

were injected immediately after fertilization, at 24 h postfertilization (hpf) and primers either for confirmation of targeted gene addition (primer1 and primer2) (A) or for *HpArs*. The PCR products were separated by gel electrophoresis. (C) RT-PCR approach using *HpMtCOI* as an internal standard. Total RNAs were extracted from 24-hpf embryos, into which indicated samples were injected, and reverse transcribed. These cDNAs were subjected to RT-PCR using primer3 and primer4 (A). (D-I) GFP expressing embryos at 30 hpf injected with *HpEts* ZFN mRNAs, the targeting donor construct and DN-lig4 mRNA. (D-F) A representative embryo showed GFP expression in primary mesenchyme cells (PMCs) viewed from vegetal pole (vv). (G-I) Another representative embryo showed GFP expression in a secondary mesenchyme cell (SMC) viewed from animal pole (av). D and G are brightfield images. E and H are fluorescent images. F and I are merged images of D-E and G-H, respectively. Arrowheads and arrows indicate GFP fluorescence in the nuclei of PMCs and a SMC, respectively. Background autofluorescences were denoted by asterisks.

Table 1. Nucleotide sequences of oligonucleotides used in this thesis

Table 1. Nucleotide sequences of oligonucleotides used in this study

Oligonucleotides	Nucleotide sequences
HpHesCF	5′–ATCTCTGCCTCTAAGGAATC–3′
HpHesCR	5′–GACAATCAACGCAATTCATC–3′
CTlig4F	5′–CTGAATTCCTGGAGGGACGAGAGCTCTGTATCATG–3′
CTlig4R	5′–CTCTCGAGTCAAGACATTGCTGCTTC*RTA–3′
HT1F	5′–AAAGCTGACATCTTGGAGATG–3′
HT1R	5′–GATGCTCTCGCAATTCGACAT–3′
ET1F	5′– ACCCAAGATGAACTACGAGAAGC –3′
ET1R	5′– GGAAAAAGCGACACTCCTCC –3′
3Z-F	5′–ACAATTGGGTAGTACGATGA–3′
3Z-R	5′–GCATCATCTCACTAGTGTGCAGAGGATCCACGCAG–3′
Random+BbsI-S	5′–GCGATCATGATCATGGAAGAC–3′
Random+BbsI-L	5′–TGGTGCAGCGTACTAGAAGACGTGTGTACGCTGGTGSNBSNBAAGSNBSNBSNBSNBGCTAAAACTCTTTCCACCAGTCTTCCATGATCATGATCGC–3′
ZF1-forward	5′–AAGGTCGTGCGGCCGGAAGACAAGCCTTACAAATGCCCAGAA–3′
ZF1-reverse	5′–CAGGACACTTATAGGGTTTTTCCCCGGTATGTGTA–3′
ZF2-forward	5′–GAAAAACCCTATAAGTGTCCT–3′
ZF2-reverse	5′–CCGGGCACTTGTATGGCTTCTCCCCGGTATGTGTA–3′
ZF3-forward	5′–GAGAAGCCATACAAGTGCCCG–3′
ZF3-reverse	5′–GACTTGTCGGCCTTGAAGACGTCTCTAGTGTGCAGAGGATCCACGCAGG–3′
pB1H2ω2-BbsI-F	5′–AGAGACTAGAAAAAGGCCGACA–3′
pB1H2ω2-BbsI-R	5′–AGGCTTCTCCCCGGGTCTAGAT–3′
delta-BsgI-L	5′–TGACACCAGTGAAGATGCGG–3′
delta-BsgI-R	5′–ACTGCTGCTGCTGCGGCAGC–3′
SSA-luc2-1	5′–ATGCGCGGTACCTAGTTATTAATAGTAATCAA–3′
SSA-luc2-2	5′–ACCGGTCCCGGGCACGACAGAGACCCTAGTCCAAGTCCACCACCTTAGC–3′
SSA-luc2-3	5′–CCCGGGTACTGATGTACCGTGAGACCTAGGAGCGCGAGCTGCTGAACAG–3′
SSA-luc2-4	5′–ATGATCTAGACTGCAGTTAAGAATTC–3′
SSA-GL4-C1C1-S	5′–GTCGGATCCAGACCCCATGACTGGGGTCTGGAGGT–3′
SSA-GL4-C1C1-A	5′–CGGTACCTCCAGACCCCAGTCATGGGGTCTGGATC–3′
SSA-GL4-C2C2-S	5′–GTCGGAAGACTCGCCCTTGACAGGGCGAGTCTGGT–3′
SSA-GL4-C2C2-A	5′–CGGTACCAGACTCGCCCAGTCAAGGGCGAGTCTTC–3′
SSA-GL4-C1C2-S	5′–GTCGGATCCAGACCCCAGAGCAGGGCGAGTCTGGT–3′
SSA-GL4-C1C2-A	5′–CGGTACCAGACTCGCCCTGCTCTGGGGTCTGGATC–3′
SSA-GL4-Ets1-S	5′–GTCGGACGTCAACCCCGTGACCGGGGTTGACGGGT–3′
SSA-GL4-Ets1-A	5′–CGGTACCCGTCAACCCCGGTCACGGGGTTGACGTC–3′
SSA-GL4-Ets2-S	5′–GTCGGAAGTCATCATCGGTGTCGATGATGACTGGT–3′
SSA-GL4-Ets2-A	5′–CGGTACCAGTCATCATCGACACCGATGATGACTTC–3′
qHpDelta-F	5′–GAGACAGCCGAGACTTGTCC–3′
qHpDelta-R	5′–CATGTAGCTCCGTTGAAGCA–3′
Ets-HRD-F	5′–ATTACTGGCAGTGGTAACAG–3′
Ets-HRD-R	5′–GACATTCTGCATGAAACCTAG–3′
2A peptide-S	5′–GAAGATCTTGCTGCCTCGAGGAGGGAAGAGGTAGCCTGCTAACTTGCGG–3′
2A peptide-R	5′–GCTCTAGAGGGACCAGGATTTTCCTCTACGTCCCCGCAAGTTAGCAGGC–3′
2A peptide-2F	5′–GAGGGAAGAGGTAGCCTGCT–3′
T3 promoter primer	5′–ATTAACCCTCACTAAAGGGA–3′
Ets HRD-inv-F	5′–TGAGAGTCCTGCAACGTGCC–3′
Ets HRD-inv-R	5′–ATCGTCGTCGCGTGCTGGAT–3′
primer1	5′–GCATCAAGGTCAACTTCAAGATCAGA–3′
primer2	5′–TGGCAAGTTTGGACAAAATTACATTC–3′
primer3	5′–GAAGTGGTCTCGAACCCTGTTATCC–3′
primer4	5′–CTTGTGGCCGAGAATGTTTC–3′

*R represents A or G

Table 2. Composition of ZFs in pc3XB vectors

	Position of ZFs		
Vectors	ZF1	ZF2	ZF3
pc3XB-ZFA36	60	64	63
pc3XB-Z1B	+BbsI	64	63
pc3XB-Z2B	60	+BbsI	63
pc3XB-Z3B	60	64	+BbsI

60, 64 and 63 represent ZF60, ZF64 and ZF63 zinc-finger domain of Zinc Finger Consortium Vector Kit v1.0,

Table 3. Nucleotide sequences of oligonucleotides used for preparation of pH3U3-B1H-reporter vectors

ZFN target site	HpHesC target subsite	Oligonucleotides		Nucleotide sequence
HpHesC1	subsite for ZF1, ZF2 and ZF3	B1HT-HesC1S	sense	5′–CCGGTGGGGTCTGGATGTC–3′
		B1HT-HesC1A	antisense	5′–AATTGACATCCAGACCCCA–3′
	subsite for ZF3	B1HT-HesC1-3S	sense	5′–CCGGAGGGGATGGTCTGTC–3′
		B1HT-HesC1-3A	antisense	5′–AATTGACAGACCATCCCCT–3′
	subsite for ZF2	B1HT-HesC1-2S	sense	5′–CCGGGGAAGTCGGTCTGTC–3′
		B1HT-HesC1-2A	antisense	5′–AATTGACAGACCGACTTCC–3′
	subsite for ZF1	B1HT-HesC1-1S	sense	5′–CCGGGGAAGATTGGATGTC–3′
		B1HT-HesC1-1A	antisense	5′–AATTGACATCCAATCTTCC–3′
HpHesC2	subsite for ZF1, ZF2 and ZF3	B1HT-HesC2S	sense	5′–CCGGAGGGCGAGTCTTGTC–3′
		B1HT-HesC2A	antisense	5′–AATTGACAAGACTCGCCCT–3′
	subsite for ZF3	B1HT-HesC2-3S	sense	5′–CCGGAGGGGATGGTCTGTC–3′
		B1HT-HesC2-3A	antisense	5′–AATTGACAGACCATCCCCT–3′
	subsite for ZF2	B1HT-HesC2-2S	sense	5′–CCGGGGAACGAGGTCTGTC–3′
		B1HT-HesC2-2A	antisense	5′–AATTGACAGACCTCGTTCC–3′
	subsite for ZF1	B1HT-HesC2-1S	sense	5′–CCGGGGAAGATGTCTTGTC–3′
		B1HT-HesC2-1A	antisense	5′–AATTGACAAGACATCTTCC–3′
HpEts1	subsite for ZF1, ZF2 and ZF3	B1HT- Ets1S	sense	5′–CCGGCGGGGTTGACGTGTC–3′
		B1HT-Ets1A	antisense	5′–AATTGACACGTCAACCCCG–3′
	subsite for ZF3	B1HT-Ets1-3S	sense	5′–CCGGCGGGGATGGTGTGTC–3′
		B1HT-Ets1-3A	antisense	5′–AATTGACACACCATCCCCG–3′
	subsite for ZF2	B1HT-Ets1-2S	sense	5′–CCGGCGAAGTTGGTGTGTC–3′
		B1HT-Ets1-2A	antisense	5′–AATTGACACACCAACTTCG–3′
	subsite for ZF1	B1HT-Ets1-1S	sense	5′–CCGGCGAAGATGACGTGTC–3′
		B1HT-Ets1-1A	antisense	5′–AATTGACACGTCATCTTCG–3′
HpEts 2	subsite for ZF1, ZF2 and ZF3	B1HT-Ets2S	sense	5′–CCGGCGATGATGACTTGTC–3′
		B1HT-Ets2A	antisense	5′–AATTGACAAGTCATCATCG–3′
	subsite for ZF3	B1HT-Ets2-3S	sense	5′–CCGGCGATGATGGTTTGTC–3′
		B1HT-Ets2-3A	antisense	5′–AATTGACAAACCATCATCG–3′
	subsite for ZF2	B1HT-Ets2-2S	sense	5′–CCGGCGAAGATGGTTTGTC–3′
		B1HT-Ets2-2A	antisense	5′–AATTGACAAACCATCTTCG–3′
	subsite for ZF1	B1HT-Ets2-1S	sense	5′–CCGGCGAAGATGACTTGTC–3′
		B1HT-Ets2-1A	antisense	5′–AATTGACAAGTCATCTTCG–3′

Table 4. Effects of injection of *HpHesC* ZFN mRNAs

ZFN mRNA	RNA (pg/embryo)	Injected embryos	Normal (%)	*HpHesC* morphant phenotype (%)	Dead (%)
$HpHesC1_{DD}$ + $HpHesC2_{RR}$	6.5 each	134	99.3	0.7	0
ZFN mRNAs	13 each	200	87	9.5	3.5
$Control\text{-}1_{DD}$ + $control\text{-}2_{RR}$	6.5 each	104	99	0	1
ZFN mRNAs	13 each	235	99.6	0	0.4

ZFN, zinc-finger nucleases.

References

Beumer, K.J., Trautman, J.K., Bozas, A., Liu, J.L., Rutter, J., Gall, J.G. & Carroll, D. (2008) Efficient gene targeting in *Drosophila* by direct embryo injection with zinc-finger nucleases. *Proc. Natl Acad. Sci*. USA 105, 19821–19826.

Cost, G.J., Freyvert, Y., Vafiadis, A., Santiago, Y., Miller, J.C., Rebar, E., Collingwood, T.N., Snowden, A. & Gregory, P.D. (2010) *BAK* and *BAX* deletion using zinc-finger nucleases yields apoptosis-resistant CHO cells. *Biotechnol. Bioeng.* 105, 330–40.

Damle, S., Hanser, B., Davidson, E.H. and Fraser, S.E., (2006) Confocal quantification of *cis*-regulatory reporter gene expression in living sea urchin. *Dev. Biol*. 299, 543–550.

Doyon, Y., McCammon, J.M., Miller, J.C., Faraji, F., Ngo, C., Katibah, G.E., Amora, R., Hocking, T.D., Zhang, L., Rebar, E.J., Gregory, P.D., Urnov, F.D. & Amacher, S.L. (2008) Heritable targeted gene disruption in zebrafish using designed zinc-finger nucleases. *Nat. Biotechnol*. 26, 702– 708.

Dreier, B., Beerli, R.R., Segal, D.J., Flippin, J.D. & Barbas, C.F. 3rd (2001) Development of zinc finger domains for recognition of the 5'-ANN-3' family of DNA sequences and their use in the construction of artificial transcription factors. *J. Biol. Chem*. 276, 29466–29478.

Dreier, B., Fuller, R.P., Segal, D.J., Lund, C.V., Blancafort, P., Huber, A., Koksch, B. & Barbas, C.F. 3rd (2005) Development of zinc finger domains for recognition of the 5'-CNN-3' family DNA sequences and their use in the construction of artificial transcription factors. *J. Biol. Chem*. 280, 35588–35597.

Dreier, B., Segal, D.J. & Barbas, C.F. 3rd (2000) Insights into the molecular recognition of the 5'-GNN-3' family of DNA sequences by zinc finger domains. *J. Mol. Biol*. 303, 489–502.

Elowitz, M.B., Levine, A.J., Siggia, E.D. & Swain, P.S. (2002) Stochastic gene expression in a single cell. *Science*. 297, 1183-1186.

Foley, J.E., Yeh, J.R., Maeder, M.L., Reyon, D., Sander, J.D., Peterson, R.T. & Joung, J.K. (2009) Rapid mutation of endogenous zebrafish genes using zinc finger nucleases made by Oligomerized Pool ENgineering (OPEN). *PLoS ONE* 4, e4348.

Frank, K.M., Sharpless, N.E., Gao, Y., Sekiguchi, J.M., Ferguson, D.O., Zhu, C., Manis, J.P., Horner, J., DePinho, R.A. & Alt, F.W. (2000) DNA ligase IV deficiency in mice leads to defective neurogenesis and embryonic lethality via the p53 pathway. *Mol. Cell* 5, 993–1002

Fujii, T., Sakamoto, N., Ochiai, H., Fujita, K., Okamitsu, Y., Sumiyoshi, N., Minokawa, T. & Yamamoto, T. (2009) Role of the nanos homolog during sea urchin development. *Dev Dyn*, 238, 2511–21

Fujiwara, A. & Yasumasu, I., (1997) Does the respiratory rate in sea urchin embryos increase during early development without proliferation of mitochondria? *Dev. Growth Differ.* 39, 179–189.

Gorski, M.M., Eeken, J.C., de Jong, A.W., Klink, I., Loos, M., Romeijn, R.J., van Veen, B.L., Mullenders, L.H., Ferro, W. & Pastink, A. (2003) The *Drosophila melanogaster DNA Ligase IV* gene plays a crucial role in the repair of radiation-induced DNA double-strand breaks and acts synergistically with Rad54. *Genetics* 165, 1929–41

Guo, J., Gaj, T. & Barbas, C.F.3rd. (2010) Directed Evolution of an Enhanced and Highly Efficient FokI Cleavage Domain for Zinc Finger Nucleases. *J. Mol. Biol.* 400, 96–107

Harborth, J., Elbashir, S.M., Bechert, K., Tuschl, T. & Weber, K. (2001) Identification of essential genes in cultured mammalian cells using small interfering RNAs. *J. Cell Sci*. 114, 4557-4565.

Hardin, J. (1996) The cellular basis of sea urchin gastrulation. *Curr. Top Dev. Biol.* 33, 159-262.

Hockemeyer, D., Soldner, F., Beard, C., et al. (2009) Efficient targeting of expressed and silent genes in human ESCs and iPSCs using zinc-finger nucleases. *Nat. Biotechnol*. 27, 851– 857.

Kurokawa, D., Kitajima, T., Mitsunaga-Nakatsubo, K., Amemiya, S., Shimada, H. & Akasaka, K. (1999) HpEts, an ets-related transcription factor implicated in primary mesenchyme cell differentiation in the sea urchin embryo. *Mech. Dev.* 80, 41–52

Levis, R., Hazelrigg, T. & Rubin, G.M. (1985) Effects of genomic position on the expression of transduced copies of the white gene of *Drosophila*. *Science*. 229, 558-561.

Maeder, M.L., Thibodeau-Beganny, S., Osiak, A., et al. (2008) Rapid ‘‘open-source’’ engineering of customized zinc-finger nucleases for highly efficient gene modification. *Mol. Cell* 31, 294–301.

Makabe, K.W., Kirchhamer, C.V., Britten, R.J. & Davidson, E.H. (1995) *Cis*-regulatory control of the *SM50* gene, an early marker of skeletogenic lineage specification in the sea urchin embryo. *Development*. 121, 1957-70.

Mandell, J.G. & Barbas, C.F. 3rd (2006) Zinc Finger Tools: custom DNA-binding domains for transcription factors and nucleases. *Nucleic Acids Res*. 34, W516–W523.

McClay, D.R., Armstrong, N.A. & Hardin, J. (1992) Pattern formation during gastrulation in the sea urchin embryo. *Dev. Suppl.* 1992, 33-41.

Meng, X. & Wolfe, S.A. (2006) Identifying DNA sequences recognized by a transcription factor using a bacterial one-hybrid system. *Nat. Protoc.* 1, 30–45.

Meng, X., Noyes, M.B., Zhu, L.J., Lawson, N.D. & Wolfe, S.A. (2008) Targeted gene inactivation in zebrafish using engineered zinc-finger nucleases. *Nat. Biotechnol.* 26, 695– 701.

Meyer, M., de Angelis, M.H., Wurst, W. & Kühn, R. (2010) Gene targeting by homologous recombination in mouse zygotes mediated by zinc-finger nucleases. *Proc. Natl Acad. Sci. USA* 107, 15022–15026.

Minokawa, T., Rast, J.P., Arenas-Mena, C., Franco, C.B. & Davidson, E.H. (2004) Expression patterns of four different regulatory genes that function during sea urchin development. *Gene Expr. Patterns* 4, 449–456.

Moehle, E.A., Rock, J.M., Lee, Y.L., Jouvenot, Y., DeKel- ver, R.C., Dekelver, R.C., Gregory, P.D., Urnov, F.D. & Holmes, M.C. (2007) Targeted gene addition into a specified location in the human genome using designed zinc finger nucleases. *Proc. Natl Acad. Sci. USA* 104, 3055–3060.

Nasevicius, A. & Ekker, S.C. (2000) Effective targeted gene 'knockdown' in zebrafish. *Nat. Genet*. 26, 216-20.

Ochiai, H., Sakamoto, N., Momiyama, A., Akasaka, K. & Yamamoto, T. (2008a) Analysis of *cis*-regulatory elements controlling spatio-temporal expression of *T-brain* gene in sea urchin, *Hemicentrotus pulcherrimus*. *Mech. Dev.* 125, 2– 17.

Ochiai, H., Sakamoto, N., Suzuki, K., Akasaka, K. & Yamam- oto, T. (2008b) The *Ars* insulator facilitates *I-SceI* meganuclease-mediated transgenesis in the sea urchin embryo. *Dev. Dyn.* 237, 2475–2482.

Okabayashi, K. & Nakano, E., (1983) The cytochrome system of sea urchin eggs and embryos. *Arch. Biochem. Biophys.* 225, 271–278.

Ramirez, C.L., Foley, J.E., Wright, D.A., Müller-Lerch, F., Rahman, S.H., Cornu, T.I., Winfrey, R.J., Sander, J.D., Fu, F., Townsend, J.A., Cathomen, T., Voytas, D.F. & Joung, J.K. (2008) Unexpected failure rates for modular assembly of engineered zinc fingers. *Nat. Methods* 5, 374–375.

Ransick, A. & Davidson, E.H. (2006) *cis*-regulatory processing of Notch signaling input to the sea urchin *glial cells missing* gene during mesoderm specification. *Dev. Biol.* 297, 587-602.

Raser, J.M. & O'Shea, E.K. (2004) Control of stochasticity in eukaryotic gene expression. *Science*. 304, 1811-1814.

Rast, J.P. (2000) Transgenic manipulation of the sea urchin embryo. *Methods Mol. Biol.* 136, 365–373.

Revilla-i-Domingo, R., Minokawa, T. & Davidson, E.H. (2004) R11: a *cis*-regulatory node of the sea urchin embryo gene network that controls early expression of *SpDelta* in micromeres. *Dev. Biol.* 274, 438-51.

Revilla-i-Domingo, R., Oliveri, P. & Davidson, E.H. (2007) A missing link in the sea urchin embryo gene regulatory network: hesC and the double-negative specification of micromeres. *Proc. Natl Acad. Sci. USA* 104, 12383–12388.

Rizzo, F., Fernandez-Serra, M., Squarzoni, P., Archimandritis, A. & Arnone, M.I. (2006) Identification and developmental expression of the *ets* gene family in the sea urchin (*Strongylocentrotus purpuratus*). *Dev. Biol.* 300, 35–48

Segal, D.J., Dreier, B., Beerli, R.R. & Barbas, C.F. 3rd (1999) Toward controlling gene expression at will: selection and design of zinc finger domains recognizing each of the 5'- GNN-3' DNA target sequences. *Proc. Natl Acad. Sci.* USA 96, 2758–2763.

Shi, Y. & Berg, J.M. (1995) A direct comparison of the properties of natural and designed zinc-finger proteins. *Chem. Biol.* 2, 83–89.

Shimizu, Y., Bhakta, M.S. & Segal, D.J. (2009) Restricted spacer tolerance of a zinc finger nuclease with a six amino acid linker. *Bioorg. Med. Chem. Lett.* 19, 3970–3972.

Shukla, V.K., Doyon, Y., Miller, J.C., et al. (2009) Precise genome modification in the crop species *Zea mays* using zinc-finger nucleases. *Nature* 459, 437–441.

Sprinzak, D., Lakhanpal, A., Lebon, L., Santat, L.A., Fontes, M.E., Anderson, G.A., Garcia-Ojalvo, J. & Elowitz, M.B. (2010) Cis-interactions between Notch and Delta generate mutually exclusive signalling states. *Nature* 465, 86-90.

Szczepek, M., Brondani, V., Büchel, J., Serrano, L., Segal, D.J. & Cathomen, T. (2007) Structure-based redesign of the dimerization interface reduces the toxicity of zinc-finger nucleases. *Nat. Biotechnol.* 25, 786–793.

Szymczak, A.L., Workman, C.J., Wang, Y., Vignali, K.M., Dilioglou, S., Vanin, E.F. & Vignali, D.A. (2004) Correction of multi-gene deficiency *in vivo* using a single 'self-cleaving' 2A peptide-based retroviral vector. *Nat. Biotechnol.* 22, 589–594

Townsend, J.A., Wright, D.A., Winfrey, R.J., Fu, F., Maeder, M.L., Joung, J.K. & Voytas, D.F. (2009) High-frequency modification of plant genes using engineered zinc-finger nucleases. *Nature* 459, 442–445.

Urnov, F.D., Miller, J.C., Lee, Y.L., Beausejour, C.M., Rock, J.M., Augustus, S., Jamieson, A.C., Porteus, M.H., Gregory, P.D. & Holmes, M.C. (2005) Highly efficient endogenous human gene correction using designed zinc-finger nucleases. *Nature* 435, 646–651.

Wolfe, S.A., Nekludova, L. & Pabo, C. (2000) DNA recognition by Cys2His2 zinc finger proteins. *Annu. Rev. Biophys. Biomol. Struct*. 29, 183–212.

Wright, D.A., Thibodeau-Beganny, S., Sander, J.D., Winfrey, R.J., Hirsh, A.S., Eichtinger, M., Fu, F., Porteus, M.H., Dobbs, D., Voytas, D.F. & Joung, J.K. (2006) Standardized reagents and protocols for engineering zinc finger nucleases by modular assembly. *Nat. Protoc.* 1, 1637–1652.

Wu, P.Y., Frit, P., Meesala, S., Dauvillier, S., Modesti, M., Andres, S.N., Huang, Y., Sekiguchi, J., Calsou, P., Salles, B. & Junop, M.S. (2009) Structural and functional interaction between the human DNA repair proteins DNA ligase IV and XRCC4. *Mol. Cell Biol.* 29, 3163–72

Yamaguchi, M.a.K.T. & Ohba, Y., (1994) Fractionation of micromeres, mesomeres, and macromeres of 16-cell stage sea urchin embryos by elutriation. *Dev. Growth Differ*. 36, 381–387.

Yamamoto, T., Kawamoto, R., Fujii, T., Sakamoto, N. & Shibata, T. (2007) DNA variations within the sea urchin *Otx* gene enhancer. *FEBS Lett.* 581, 5234–5240.

Yamazaki, A., Ki, S., Kokubo, T. & Yamaguchi, M. (2009) Structure-function correlation of micro1 for micromere specification in sea urchin embryos. *Mech. Dev.* 126, 611– 623.

Yáñez, R.J. & Porter, A.C. (1999) Gene targeting is enhanced in human cells overexpressing *hRAD51*. *Gene Ther*. 6, 1282–1290.

Yoo, S.H., Yamazaki, S., Lowrey, P.L., Shimomura, K., Ko, C.H., Buhr, E.D., Siepka, S.M., Hong, H.K., Oh, W.J., Yoo, O.J., Menaker, M. & Takahashi, J.S. (2004) PERIOD2::LUCIFERASE real-time reporting of circadian dynamics reveals persistent circadian oscillations in mouse peripheral tissues. *Proc. Natl Acad. Sci.* USA 101, 5339-5346.

Zou, J., Maeder, M.L., Mali, P., Pruett-Miller, S.M., Thibodeau-Beganny, S., Chou, B.K., Chen, G., Ye, Z., Park, I.H., Daley, G.Q., Porteus, M.H., Joung, J.K. & Cheng, L. (2009) Gene targeting of a disease-related gene in human induced pluripotent stem and embryonic stem cells. *Cell Stem Cell* 5, 97–110.

Acknowledgements

The author would like to express his deepest appreciation for his major professor, Dr. Takashi Yamamoto, for providing an understanding environment to complete his thesis studies. The author would also like to thank Dr. Naoaki Sakamoto and Dr. Tatsuo Shibata for the helpful suggestions and their timely advice. Sincere appreciation is also extended to Dr. Ken-ichi Suzuki, Dr. Masatoshi Nishikawa, Dr. Sumihare Noji, Dr. Shinya Matsuura, Dr. Tatsuo Miyamoto and Dr. Koji Akasaka for fruitful discussions. I am grateful to members of Dr. Takashi Yamamoto laboratory for discussions. The author also wish to express their thanks to Dr. Keith Joung for providing the pST1374 expression vector (Addgene plasmid 13426), Dr. Daniel Voytas for supplying the pc3XB-ZF60, pc3XB-ZF63, pc3XB-ZF64 and pc3XB-ZF70 vectors (Addgene plasmid 13196, 13199, 13200 and 13193, respectively), Dr. Scot Wolfe for providing the pH3U3-mcs reporter vector, pB1H2x2-zif268 plasmid and US0*ΔhisBΔpyrFΔrpoZ* bacterial strain (Addgene plasmids 12609, 184045 and 18049, respectively) and Dr. Masato Kiyomoto for supplying live sea urchins. The author also thank the Fisheries and Ocean Technology Center, Hiroshima Prefectural Technology Research Institute for supplying seawater. I also thank to the Cryogenic Center of Hiroshima University for supplying liquid nitrogen. This study was supported by a Grant-in-Aid for Scientific Research on Innovative Areas (No. 2020006) to T.Y. and a Grant-in-Aid for JSPS Fellows (No. 09J01990) to H.O.